

Observations on the Influence of Tool-Sheet Contact Conditions on an Incremental Forming Process

M. Durante, A. Formisano, and A. Langella

(Submitted December 17, 2009; in revised form January 4, 2010)

The influence of tool-sheet contact conditions on features such as surface roughness, forming force, and formability was evaluated for components produced by incremental forming, a highly flexible innovative sheet metal-forming process. Experimental tests were carried out on sheets of AA7075T0 to create two types of component: pyramid frusta (for the evaluation of roughness and force) and cone frusta (for the evaluation of formability). Four different types of tool-sheet contact were analyzed, using two types of tool. From the experimental tests, the influence on the surface finishing and on the trend of the forming forces depending on contact type was revealed. Contact types do not, however, influence sheet formability.

Keywords formability, forming force, incremental forming, roughness

1. Introduction

Incremental forming is a technology that presents some relevant limitations with respect to traditional sheet metal-forming processes, like the high manufacturing time and the lack of geometrical accuracy (both in macroscopic and in microscopic terms) of the formed parts. In particular, surface roughness in incremental forming is regarded as a weak point when compared to the traditional processes. Moreover, the max wall angle of the components is limited and the forming forces can create problems for the machines, since they are not dedicated to the process in exam. On the other hand, this process allows reducing set-up costs significantly and presents a very high flexibility; it is, in fact, possible to create different components simply by operating on the tool path with the same tool. Relatively to this latter, the punch with the hemispherical head turned out to be the most commonly used in the incremental forming processes, whereas the sphere was used in few works.

Studies on the geometrical accuracy of components produced by incremental forming were conducted in the past, but were aimed mainly at evaluating the gap between the experimental profile and the one designed. Macroscopic evaluations were then made to identify the principal causes of these discrepancies and to optimize the process parameters to improve conformity. The need thus arose to evaluate the geometrical quality of the components produced using incremental forming, in microscopic terms as well, and then the

choice of the roughness evaluation. Hagan and Jeswiet (Ref 1) highlighted the importance of the roughness, especially for automotive parts. In their studies, they described the surface finishing in incremental forming as a combination of large-scale waviness resulting from the tool path and small-scale roughness resulting from the large surface strains; it resulted that as the vertical tool step decreases, the surfaces show to transform from wavy to strictly roughness without waviness. Furthermore, the tool rotation speed does not influence the roughness. Junk et al. (Ref 2) studied the effect of the wall angle, the vertical step, and the tool radius; relatively to the influence of the latter two parameters, they observed an increase of roughness with the vertical step and a decrease with the diameter.

Regarding the forming force, Duflou et al. (Ref 3) highlighted that the global force (that is the combination of the vertical and the two horizontal components) increases with the increase in vertical step, tool diameter, wall angle of the geometries, and sheet thickness. Durante et al. (Ref 4), in a work in which use of the sphere was not considered and the diameter and the step were not varied, emphasized that the vertical component of the forming force is not significantly affected by the different contact conditions. Similarly, this is true for the horizontal component along the direction of tool movement, while rotation brings about different behavior for the horizontal component along the direction of tool movement only, given that it is closely linked to friction.

Finally, the evaluation of sheet formability acquired key relevance, given that it furnishes indications on the geometrical limits of the components. Kim and Park (Ref 5) found an optimum tool diameter for maximum formability and a slight increase in formability following the use of the non-lubricated sphere, in comparison with the punch with the hemispherical head; Park and Kim (Ref 6) showed that formability increases as tool radius increases or vertical feed decreases. In both the cases, the straight groove test was used. Differently, circular profiles were used to test the thinning limits in incremental forming (Ref 7-9).

In the light of what was above-mentioned, it is clear that the current state-of-the-art does not cover all the aspects of this innovative technological process; consequently, the aim of the following work is to broaden and deepen the knowledge related

M. Durante, A. Formisano, and A. Langella, Department of Materials and Production Engineering, University of Naples, Federico II, Piazzale Tecchio 80, 80125 Naples, Italy. Contact e-mail: aformisa@unina.it.

to the influence of tool-sheet contact type on sheets formed using an incremental forming process, to optimize the choice of the tool type and the combination of the process parameters depending on the features of greater interest. In this manner, it is possible to control important targets, like surface roughness, forming force and formability, and this allows to better understand the limits of the process.

Four contact types were analyzed, three of them using a punch with a hemispherical head (not rotating and rotating, in both directions) and one using a freely rotating sphere. The experimental campaign was carried out on aluminum alloy sheets, for the different contact types and by varying the tool diameter and the vertical tool step.

2. Experimental Tests

In order to create the different tool-sheet contact conditions, two tool types were used, a sphere and a cylindrical punch with hemispherical head, both made of steel (Fig. 1).

The first one can rotate freely into a cave, covered with a thin layer of Teflon, positioned on the top of the cylindrical styli that drives it; the latter was tested both unrotating and at a rotation speed of 600 rpm, and in both clockwise and in anticlockwise directions. In all the tests using the punch with the hemispherical head, the sheet was lubricated with a thin layer of oil to avoid abrasion and its consequent failure, whereas only the contact zone between the sphere and the cave was lubricated. Sliding tests, proposed for the evaluation of the friction coefficients (Ref 4), furnished the following values: 0.19 at 0 rpm, 0.06 at 600 rpm, and 0.04 for the contact type with the sphere. Three different tool diameters were tested: 5, 10, and 15 mm.

Sheets of AA7075T0, 1 mm thick, were adopted. This alloy, used in the field of aerospace for structural applications, has the following mechanical characteristics: Young modulus $E = 75$ GPa, yield strength $Y = 100$ MPa, ultimate tensile strength $UTS = 200$ MPa, and percent elongation $\epsilon_r = 22\%$. In all the tests, carried out by means of a high speed four-axis vertical machining center C. B. Ferrari, the tool describes the path in an anticlockwise direction, with a feed of 1000 mm/min. The equipment used for producing the components, described below, is shown in Fig. 2.



Fig. 1 Tool types

Two types of geometry were chosen, depending on the features to be evaluated: a pyramid frustum for the evaluation of roughness and forming force, and a cone frustum with circular profile for the evaluation of sheet formability.

The pyramid frusta were produced by a spiral path consisting of square coils. This type of geometry was chosen because the flat faces allow easy acquisition of roughness measurements and, moreover, the linear segments of the tool path mean that the force components connected with forming can easily be told apart from those connected to friction. The tests were conducted by adopting three different vertical step values of 0.2, 0.4, and 0.6 mm. A qualitative representation of the tool path, where O represents the starting point, is shown in Fig. 3. A slope angle of 60° (Ref 10) and a frustum base length of 80 mm were chosen. The height of the pyramid frusta is 40 mm.

For the evaluation of the formability, cone frusta with a circular profile were chosen. With this choice, rather than a series of cones with increasing wall angle, it is possible to investigate, in one only test, the wall angle by varying it with continuity. The cone frusta were produced starting with a spiral path made up of circular coils (Fig. 4a) using angular steps of 0.5° , 1° and 1.5° ; the geometrical features of the profile are shown in Fig. 4b.

Relatively to the roughness, two parameters were examined: the average roughness (R_a) and an index of max roughness (R_z). These two parameters were chosen because R_a is widely used as a parameter for the surface finishing, while R_z rather than R_t

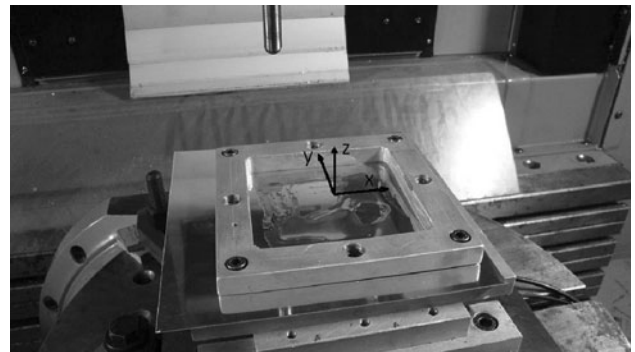


Fig. 2 The sheet-forming equipment

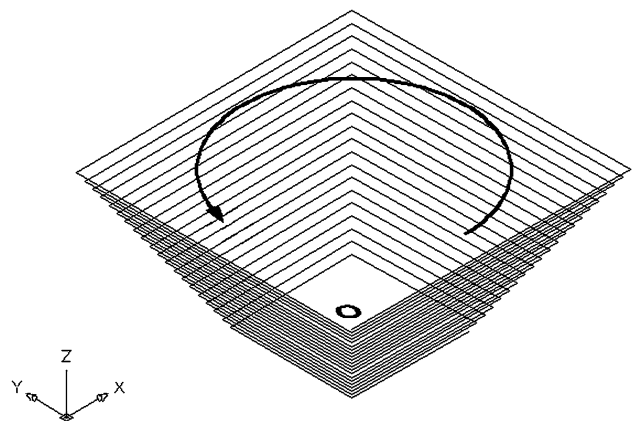


Fig. 3 Qualitative representation of the tool path for the creation of pyramid frusta

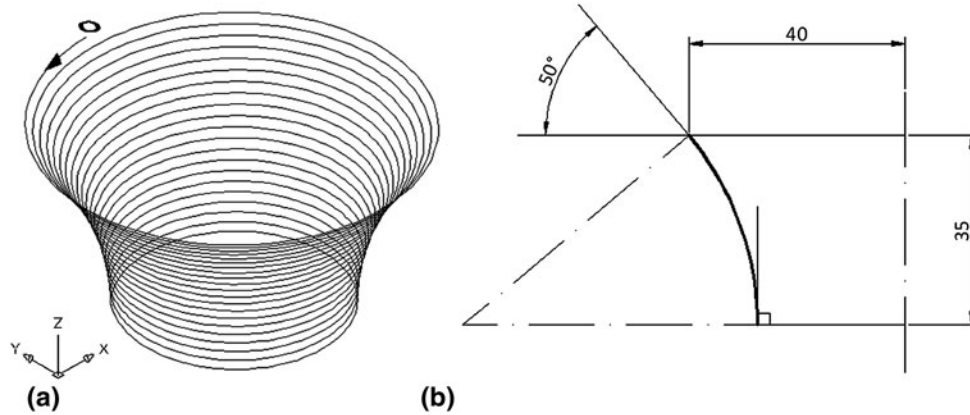


Fig. 4 Qualitative representation of the tool path for the creation of cone frusta (a) and geometrical features of the frustum (b)

(that is the maximum distance between the highest peak and the lowest groove of the roughness profile) was chosen, to prevent any accidental surface irregularity from influencing the experimental evaluation of the roughness. In fact, R_t represents the maximum height of the profile, R_z is the average of this feature, evaluated on ten points. The two roughness parameters were measured perpendicular to the direction of the tool movement, by a Rugosimeter “Surftest SJ-301” with differential inductance used as the detecting method and with gaussian filter. Measures with different cut-off values were carried out to follow the indications furnished by ISO 4288-1996 standard relatively to the recommended cut-off values for periodic profiles (that is the scallops create by the tool path); in the light of simple geometrical considerations, a value of the period equal to $p/\sin\alpha$ (where p represents the vertical step and α the wall angle of the frusta) was chosen. A full experimental campaign was carried out and ten measures were recorded for each test. The ten measurements were divided equally over two contiguous internal faces of the pyramid frusta to avoid casual errors linked to any anisotropic behavior in terms of sheet roughness.

The evaluation of the forming force, conducted on the same experimental campaign of the roughness evaluation, was made possible by the use of a two channel load cell; the measurement accuracy is 0.1 N. One channel provides the vertical component F_z , whereas the other provides the horizontal component F_x (in the global coordinate set x , y , and z shown in Fig. 2). From the only horizontal component measured it was possible to analyze the tangential (F_t) and the radial (F_r) components, respectively, locally parallel and perpendicular to the tool movement. After an initial number of coils, necessary to reach the final tool-sheet contact conditions, the force components demonstrated a typical trend as shown in Fig. 5. The fact that the horizontal force is a mirror image about the time axis for the first two (labelled 1 and 2) and the last two sides (labelled 3 and 4) of the pyramid confirms that the load cell was correctly calibrated. It must be pointed out that the considerations in terms of force were made only for the trends of the components, and not for the peaks (that are presents in Fig. 5 in correspondence to the corners of the pyramid frusta).

The evaluation of formability was carried out by evaluating the angle corresponding to where sheet failure occurs on varying the contact conditions. Then, the choice fell on the formability angle, which was also chosen by Capece Minutolo et al. (Ref 10) for the same material. The decision not to carry

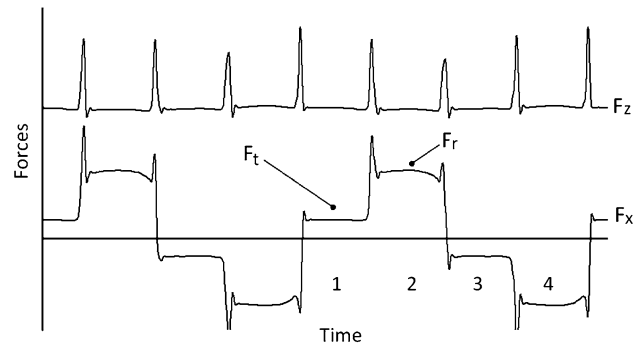


Fig. 5 Trend of the forming force components

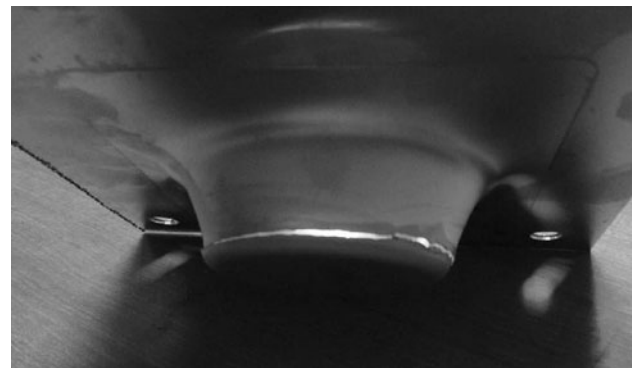


Fig. 6 Sheet failure at the level of the max formability angle

out the straight groove test is due to the fact that this test does not accurately reproduce the process examined and, moreover, requires us to obtain deformation in a way that is far from simple, to describe formability in the forming limit diagrams. Indeed, this test requires forming on one only side of the sheet and, in addition, the measurement of minor and major strains of deformed grids etched onto or attached to the specimen, near the zone where the failure appears; this zone turns out to be somewhat peculiar, as it is an end of the tool path. The lack of geometrical singularities and the description of a spiral path (not with discrete steps) meant not that localized failures could be obtained, but that the tool path could go on following the occurrence of said failures (Fig. 6).

However, it is important to underline that the maximum wall angle represents a process capability which may be dependent on factors not investigated in this work like, e.g., the starting diameter of the cone frusta.

3. Results

The results for roughness, forming force, and formability are presented, respectively, in Section 3.1 to 3.3.

3.1 Roughness

The geometrical and experimental roughness profiles for a generic test are shown in Fig. 7, whereas the graphs of the two roughness parameters are shown in Fig. 8 (the values shown represent the averages of the ten measurements for each test). The values for all the tool-sheet contact types were evaluated depending on the step and for the various diameters.

It is possible to observe that both the roughness parameters show the highest values for the punch with the nonrotating hemispherical head, whereas a decrease is seen when the punch

is set in rotation. The direction of rotation turns out to be negligible, so that the two curves frequently overlap. These results were already noted in a work on only one combination of the parameters (Ref 4). Now, on the other hand, it is possible to affirm that those results also hold true when the parameters analyzed are varied. The roughness shows a decrease when the sphere is used. This result means that the most marked stroke is generated by using the punch with a nonrotating hemispherical head (in most cases, for this contact type, the roughness is almost half as much again as the value using the sphere but it is possible to observe that in some cases it is almost twice). The experimental profile (that respects the periodicity of the geometrical one) shows that the scallops are not pure geometrical, but there is an influence of friction coefficient. In fact, the roughness decreases with the increase in friction coefficient, presumably because the mechanism is more similar to the shear for tool not rotating (highest friction coefficient value) than for the sphere (lowest friction coefficient value). The rotating tool takes up an intermediate position respect to the two above-mentioned contact types.

As regards the absolute roughness values, they are very low; the majority of the R_a values are, in fact, included in the category of the surfaces obtained by machining or hand grinding, with reference to ISO 4287/1. Moreover, for the conditions in which the roughness has the lowest values (step 0.2 mm and diameter 15 mm), these are comparable to the blank ones, that is 0.32 and 1.6 μm for R_a and R_z , respectively.

3.2 Forming Force

With the use of the sphere, the friction coefficient decreases and this involves a decrease in F_t when compared with the nonrotating punch, although values are higher when compared

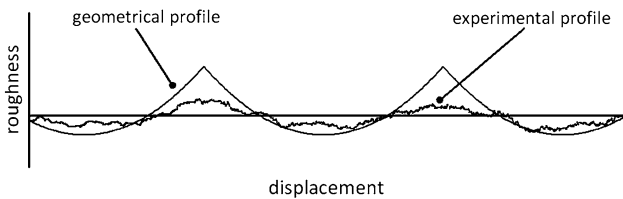


Fig. 7 Geometrical and experimental roughness profiles

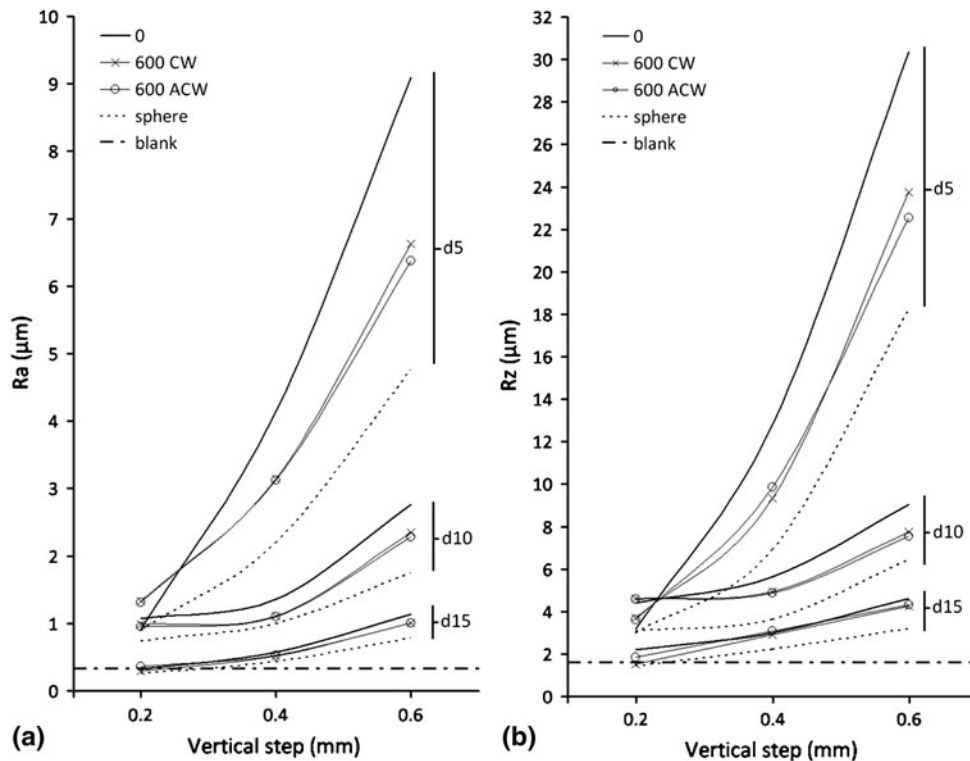


Fig. 8 Average (a) and Max surface roughness (b) versus vertical step

with those ones with the punch rotating in clockwise direction, as a result of the punch-sheet relative motion. Differently, F_r and F_z are influenced minimally by contact type (Fig. 9a). It is worth pointing out that F_r and F_z are the force components that create the forming, whereas F_t can be associated to the step of material to be deformed and the friction force.

Moreover, it is possible to observe that both F_r and F_z increase with step and diameter, so as Duflou et al. (Ref 3) highlighted relatively to the global force, whereas F_t increases with step and decreases with diameter (Fig. 9b, regarding use of the sphere). The increase of F_r and F_z with step depends on the augment of material to deform. Relative to F_t , the vertical step to be flattened for two subsequent path coils increases with the step (p), since the arc of contact increases (Fig. 10a). Increasing the diameter (d), on the other hand, the contact area between punch and sheet increases, and thus we have an obvious increase in the forming components, F_r and F_z ; F_t decreases, however, since the flattening of the feed rate becomes less accentuated, due to a reduction in the arc of contact (Fig. 10b).

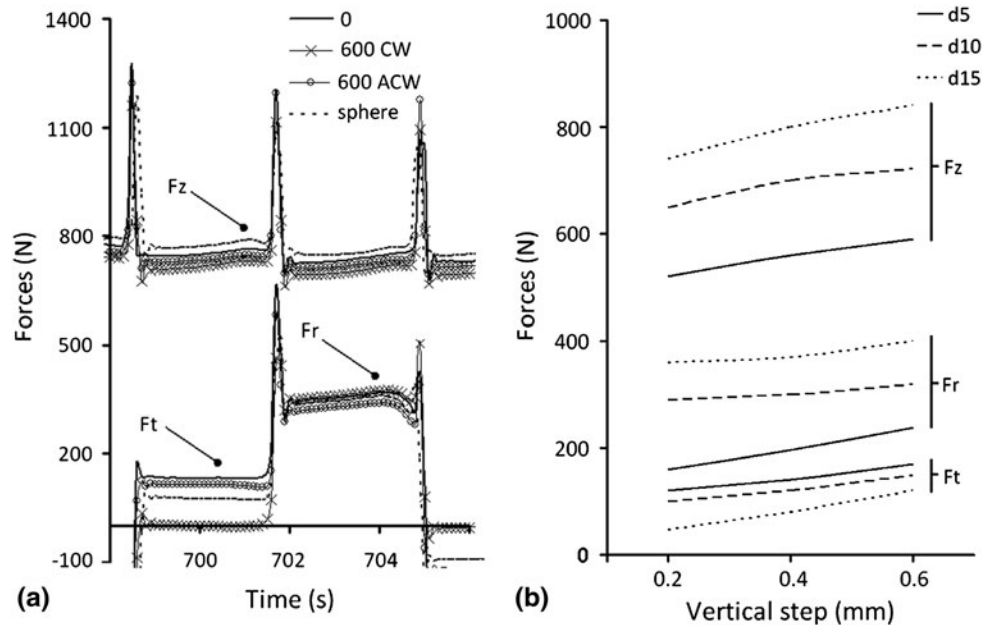


Fig. 9 Forming force components varying the contact conditions (a) and the step for different diameters (b)

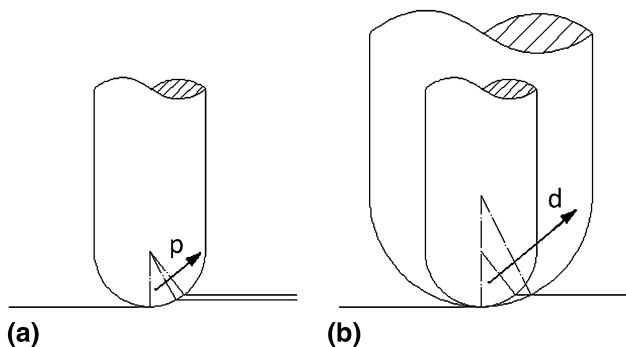


Fig. 10 Contact conditions varying the step (a) and the diameter (b)

3.3 Formability

The evaluation of the angle at the level at which the failure occurs was not influenced significantly by the tool-sheet contact type, because values of between 72° and 73° were measured in all the cases with diameter of 10 mm and angular step of 0.5° . This result is strengthened by the fact that the change in thickness, rather than depending on the roughness (because of the little values of the same), can be predicted by the Cosine law ($t = t_0 \cos\alpha$, where t and t_0 are, respectively, the thickness of the formed and undeformed sheet), according to Wei et al. (Ref 11).

As a consequence, formability does not vary with contact type, and the other tests were conducted for only one contact type, that is the punch not rotating, to reduce the number of tests. It was noted that the formability decreases both with the diameter and the angular step (Fig. 11); in the light of this, the formability decreases with the increase of the tool-sheet contact area, since there is a minor local deformation mechanism. The result, only relatively the influence of the tool diameter, is in contrast with (Ref 5, 6) that used the straight groove test.

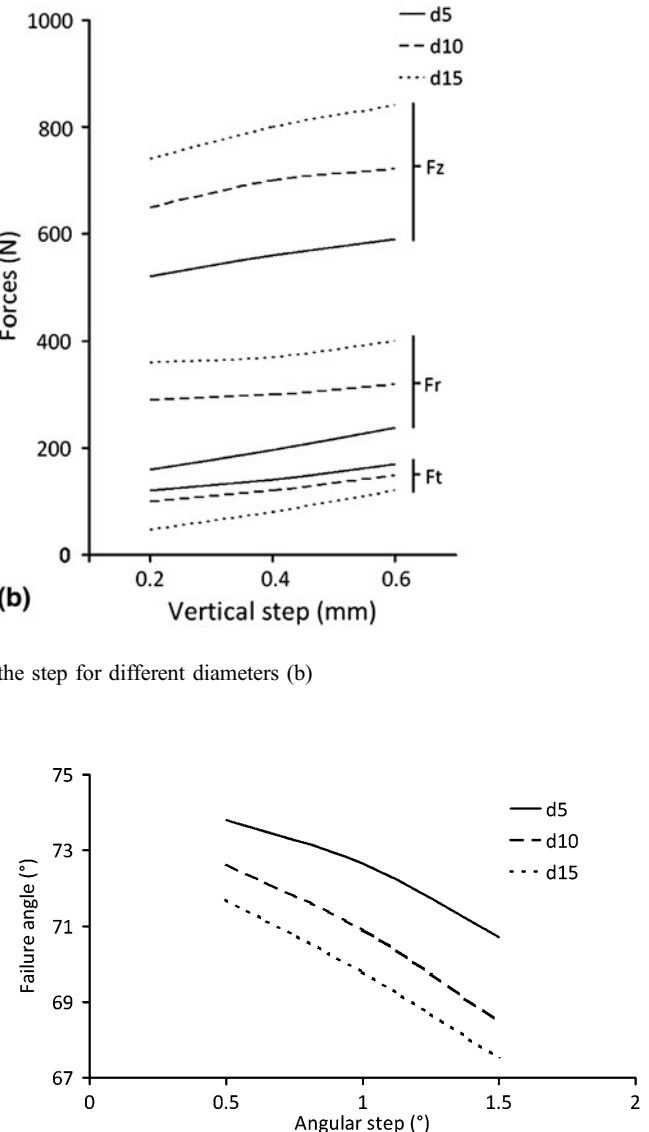


Fig. 11 Failure angle varying the angular step for different diameters

4. Conclusions

The aim of this study is to provide information on the roughness, in terms of R_a and R_z , on the components of the forming force and on the formability regarding components produced using an incremental forming process, by varying the tool-sheet contact type, to deepen the knowledge on this innovative sheet metal-forming process. For this reason, an experimental campaign was carried out on pyramid and cone frusta, produced from sheets of AA7075T0 and for four contact types.

With regard to surface roughness, the contact with the punch with the nonrotating hemispherical head was the one that gave the highest levels of roughness, while the lowest levels were recorded with sphere-sheet contact. In quantitative terms, it was observed that the lowest values of the roughness are almost equal to that of the blanks, whereas the highest ones remain within technologically acceptable limits.

As regards the analysis of the forming force, it was noted that the two components strictly connected to the forming do not depend noticeably on the different punch-sheet contact conditions, whereas they demonstrate a direct dependence on the step of the path and the diameter of the tool. Different considerations were made for the component connected to friction, as it is strongly influenced by the contact type, showing a proportional dependence on the vertical step, and an inverse one on tool diameter.

Formability, evaluated by measuring the maximum forming angle for the cone frusta with circular profile, decreases with the tool diameter and the angular step, whereas turns out not to be influenced by the contact type.

References

1. E. Hagan and J. Jeswiet, Analysis of Surface Roughness for Parts Formed by Computer Numerical Controlled Incremental Forming, *Proc. Inst. Mech. Eng. B*, 2004, **218**, p 1307–1312
2. S. Junk, G. Hirt, and I. Chouvalova, Forming Strategies and Tools in Incremental Sheet Forming, *Proc. 10th Int. Conf. Sheet Met.* (Shemet), Ulster, Ireland, April 2003, p 57–64
3. J. Dufflou, A. Szekeres, and P. Vanherck, Force Measurements for Single Point Incremental Forming: An Experimental Study, *Proc. 11th Int. Conf. Sheet Met.* (Shemet), Erlangen-Nuremberg, Germany, April 2005, p 441–448
4. M. Durante, A. Formisano, A. Langella, and F. Capece Minutolo, The Influence of Tool Rotation on an Incremental Forming Process, *J. Mater. Process. Technol.*, 2009, **209**, p 4621–4626
5. Y.H. Kim and J.J. Park, Effect of Process Parameters on Formability in Incremental Forming of Sheet Metal, *J. Mater. Process. Technol.*, 2002, **130–131**, p 42–46
6. J.J. Park and Y.H. Kim, Fundamental Studies on the Incremental Sheet Metal Forming Technique, *J. Mater. Process. Technol.*, 2003, **140**, p 447–453
7. G. Hussain, L. Gao, and N.U. Dar, An Experimental Study on Some Formability Evaluation Methods in Negative Incremental Forming, *J. Mater. Process. Technol.*, 2007, **186**, p 45–53
8. G. Hussain, N.U. Dar, L. Gao, and M.H. Chen, A Comparative Study on the Forming Limits of an Aluminum Sheet-Metal in Negative Incremental Forming, *J. Mater. Process. Technol.*, 2007, **187–188**, p 94–98
9. G. Hussain and L. Gao, A Novel Method to Test the Thinning Limits of Sheet Metals in Negative Incremental Forming, *Int. J. Mach. Tool Manuf.*, 2007, **47**, p 419–435
10. F. Capece Minutolo, M. Durante, A. Formisano, and A. Langella, Evaluation of the Maximum Slope Angle of Simple Geometries Carried Out by Incremental Forming Process, *J. Mater. Process. Technol.*, 2007, **194**, p 145–150
11. H.Y. Wei, L. Gao, and S.G. Li, Investigation on Thickness Distribution Along Bulge Type Incrementally Formed Sheet Metal Part With Irregular Shapes, *Proc. Int. Manuf. Conf.*, Jinan, China, September 2004, p 1672–3961 (Supp-01)